Experimental and Numerical Investigation of the Flow Past a Thin Circular Airfoil with Mid-Chord Slot

Assist. Prof. PhD Eng. **Andrei DRAGOMIRESCU**[1], Prof. PhD Eng. **Carmen-Anca SAFTA**[2], Assoc. Prof. PhD Eng. **Marius STOIA-DJESKA**[3]

[1] University Politehnica of Bucharest, Department of Hydraulics, Hydraulic Machinery and Environmental Engineering, andrei.dragomirescu@upb.ro

[2] University Politehnica of Bucharest, Department of Hydraulics, Hydraulic Machinery and Environmental Engineering, carmen-anca.safta@upb.ro

[3] University Politehnica of Bucharest, Department "Elie Carafoli" of Aerospace Science, marius.stoia@gmail.com

Abstract: *Results of an experimental and numerical study of the flow past thin, circular arc cambered airfoils with a narrow slot at mid-chord are presented in this paper. The purpose of the study was to investigate the aerodynamic characteristics of this type of airfoils from the point of view of using them in the aerodynamic structure of a small wind turbine. The experimental study was carried out in a closed (return-flow) wind tunnel. Drag forces were measured at different Reynolds numbers for airfoils having slots of different widths, placed at a constant angle of attack of 90°. The numerical study was extended to similar airfoils intended to be used for the guide vanes of a small cross-flow wind turbine. The results of the study show that the usage of mid-chord narrow slots could significantly reduce the aerodynamic loads on the guide vanes of the wind turbine.*

Keywords: *slotted airfoil, aerodynamic loads, wind turbine, guide vanes, CFD*

1. Introduction

The development of the boundary layer was intensively studied for decades due to the fact that the viscous shear stresses that appear inside it and its separation are crucial for determining lift and drag of wings. Different techniques to control the boundary layer were developed to increase the lift or to decrease the drag [1]. Boundary layer control is applied for phenomena of transition from a laminar boundary layer to a turbulent one or in the case of boundary-layer separation [2]. Both in case of transition and of separation suction can be applied as a method of boundary layer control. A very simple, yet very effective suction control is by using properly placed slots that link the pressure side of a wing to its suction side. The pressure difference drives the fluid through such a slot towards the suction surface. The additional fluid flow injected in this manner at a specific position on the suction surface can delay or even cancel the boundary layer separation, thus improving the lift of the airfoil. Such slots are usually placed either close to the leading edge or close to the trailing edge of the wing.

In this study it was aimed actually not at increasing but at decreasing the lift of an airfoil in order to decrease the loads on the guide vanes of a cross-flow wind turbine having a runner similar to those studied by Dragomirescu [3] and Dragomirescu et al. [4]. Preliminary experimental tests showed that by placing the slot at mid-chord could reduce the aerodynamic loads on the airfoil. A numerical study was subsequently carried out in order to get a better insight into the flow around the airfoil and to extend the experimental results.

In the following, the experimental and numerical studies are presented. Obtained results are discussed and, based on them, conclusions are drawn.

2. Experimental Setup

The experimental study was performed in a subsonic wind tunnel with return-flow and with an open test section (Fig. 1). The wind tunnel is powered by a fan driven by a variable DC motor, so that the maximum air velocity provided in the test section (without any blockage) is of about 30 m/s. Upstream of the test section, the flow is directed into a setting chamber containing screens for
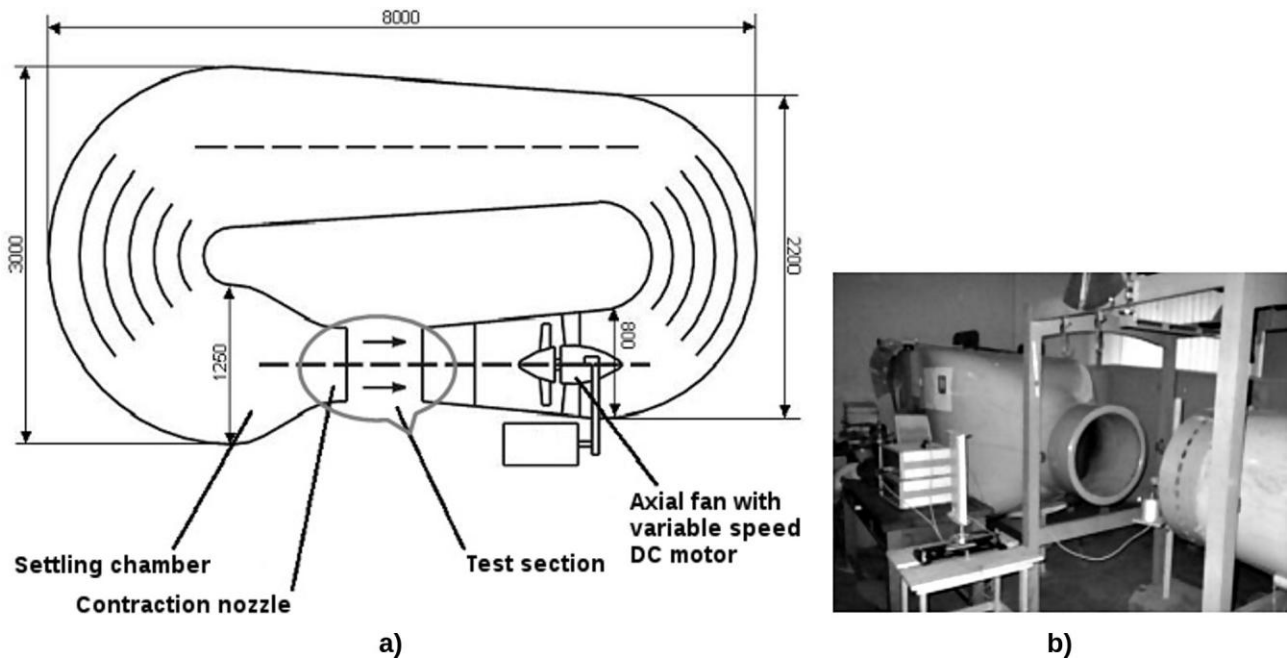
a)   b)

Fig. 1. Experimental installation: a) sketch of the subsonic wind tunnel in "Nicolae Tipei" Laboratory at Department "Elie Carafoli" of Aerospace Science and b) photo of the test section.

reducing turbulence and a contraction nozzle downstream to further reduce turbulence and to accelerate the flow to test velocity. The flow in the open test section is nearly uniform with low turbulence levels.

In this wind tunnel, different arc-shaped thin airfoils with slots at mid-chord were tested. The geometry of the airfoils is presented in Fig. 2. Chord length and breadth of airfoils were kept constant at 45 mm and 60 mm respectively. The slots had a constant length of 50 mm, while their width, *b*, was changed from 0 mm (i.e. no slot) to 6 mm, 8 mm, 10 mm, and 12 mm. The airfoil without slot (with *b* = 0 mm) will be further referenced as *normal airfoil*.

The methodology of testing consisted in measuring drag forces on the airfoil by using a three-component force sensor placed beneath the test section. As it can be seen in Fig. 3, the experimental airfoil (1) is fixed through the support link (3). The force sensor (2) is of type HM 170.40 GUNT [5]. The sensor is connected to an electronic amplifier with digital displays for lift, drag, and aerodynamic pitching moment. A graduated scale allows setting the airfoil at the desired angle of attack.
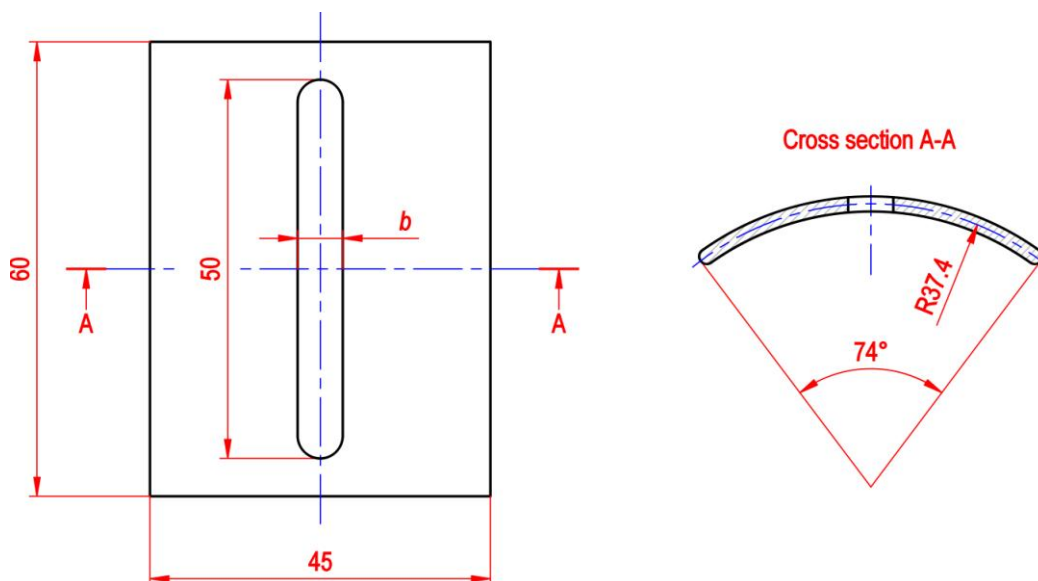

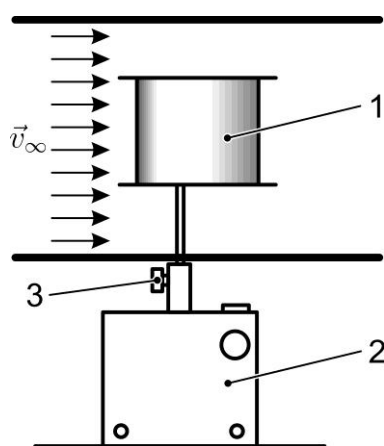**Fig. 2.** Sketch of the experimentally investigated airfoil with mid-chord narrow slot.

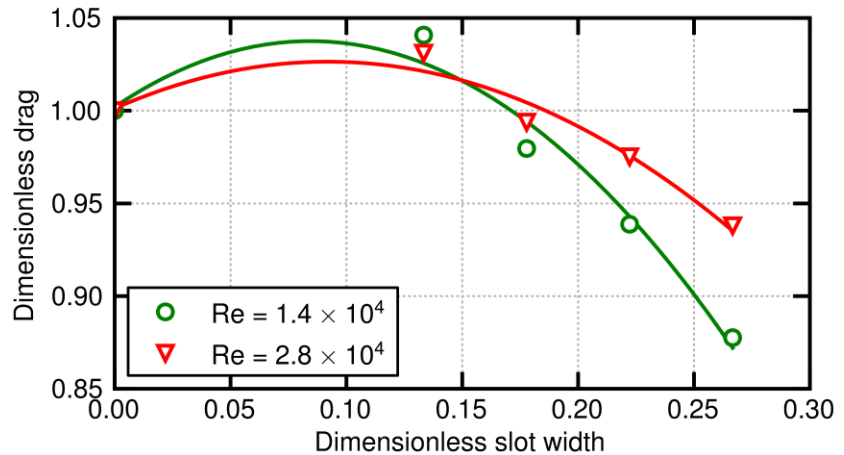**Fig. 3.** Assembly of tested airfoil on force sensor.

Fig. 4. Variation of dimensionless drag depending on dimensionless slot width.

The experiments aimed at finding the variation of drag force depending on slot width at different air velocities, i.e. at different Reynolds numbers. The angle of attack was kept constant, $\alpha = 90^0$. Measurements were carried out at air velocities v_∞ of 5 m/s and 10 m/s, for which the Reynolds numbers are of about 1.4×10^4 and 2.8×10^4 respectively. The Reynolds numbers were calculated based on the chord length of 45 mm and on the air kinematic viscosity that at test conditions has the value of 1.581×10^{-5} m^2/s.

The experimental results are summarized in Fig. 4 in form of variations of dimensionless drag force depending on dimensionless slot width. At each Reynolds number the reference force is the drag measured on the normal airfoil. The reference length is the chord length. The results obtained suggest that for very narrow slots the drag increases slightly. However, as the dimensionless slot width increases above 0.15, the drag starts to decrease. This decrease becomes less steep as the Reynolds number increases.

3. Numerical Simulations

In order to get an insight into the flow past the circular arc airfoil, numerical simulations were performed for different Reynolds numbers and angles of attack both for the slotted airfoil and for the normal airfoil. The airfoils studies were designed to be used in a cascade of guide vanes for a cross-flow wind turbine having the runner diameter of 1.2 m. At entry and exit of the cascade the blade angles are of 90° and 16° respectively. The outer and inner diameters of the cascade are of 1.79 m and 1.38 m respectively. Fig. 5 presents the resulting slotted airfoil and its dimensions. The chord length is of 235 mm. The slot is placed at mid-chord and has a width of 3 mm. Its axis is
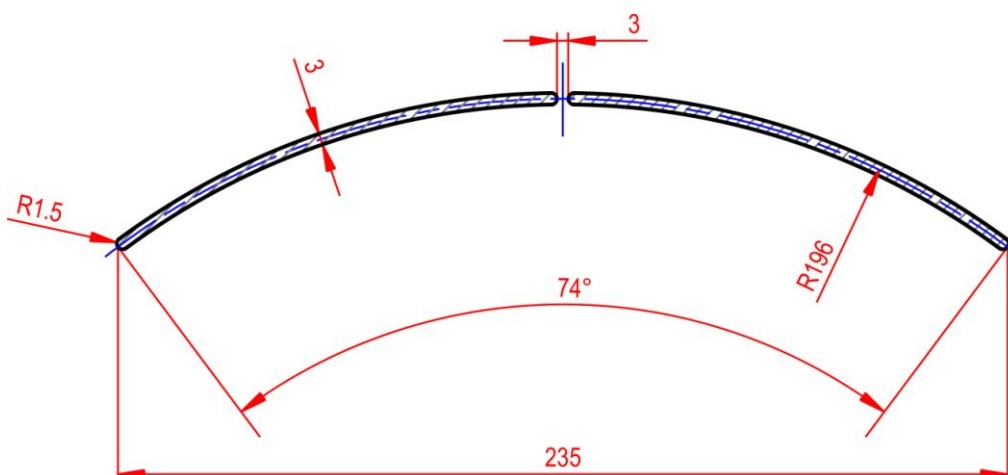

Fig. 5. Sketch of the airfoil with narrow slot, studied by numerical simulations.
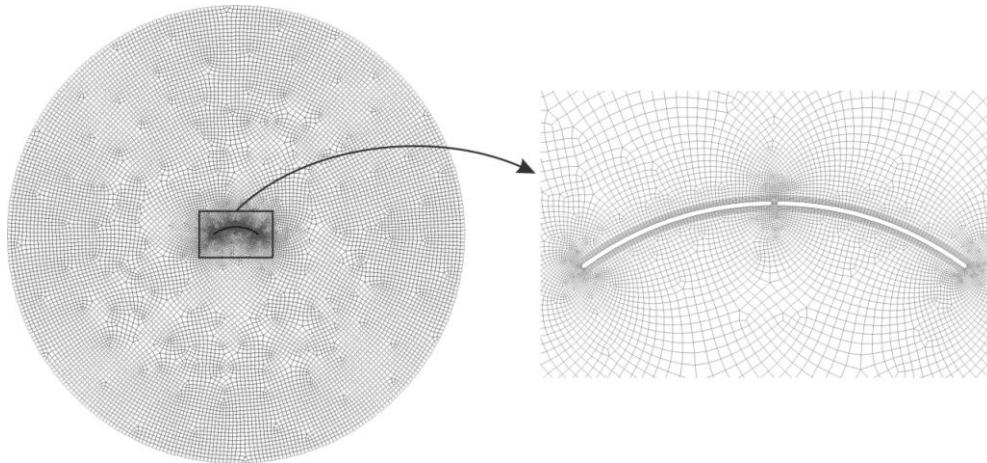
Fig. 6. Computational domain and mesh.

perpendicular to camber line. The normal airfoil has similar geometry and dimensions, except that it has no slot.

For both airfoils the numerical simulations were performed on the two-dimensional computational domain presented in Fig. 6. The domain is circular and has a diameter of 2.4 m, which is roughly ten times higher than the chord length. The airfoils were placed in the middle of this domain. The domain was meshed using quadrilateral cells that form an unstructured grid. Boundary layer-type cells were used close to the airfoils. The resulting grid is also presented in Fig. 6.

The working fluid is air at the reference pressure $p_0 = 10^5$ Pa and the reference temperature $T_0 = 293.15$ K. The air was considered an ideal gas having a constant dynamic viscosity of 1.824×10^{-5} Pa s.

As it will be detailed later, the Reynolds numbers of the flow past the airfoils are relatively large. Additionally, it was desired to catch the effect of the vortices that detach behind the airfoils, in case that these vortices appear. Therefore, the air flow was treated as unsteady and turbulent, being described by the continuity and the Reynolds averaged Navier-Stokes (RANS) equations. The closure equations for the turbulent stresses were provided by the Reynolds Stress Model (RSM) with standard wall functions. This turbulence model was chosen because it is considered to be one of the most elaborate turbulence models, having a great potential to give accurate predictions for complex flows [6].

Numerical simulations were performed for two velocities v_∞ of the free air stream and different angles of attack α of the airfoils. In order to easily change the angle of attack without changing the geometry and re-meshing the computational domain, the outer boundary was treated as a pressure far-field boundary. Consequently, gauge pressure, Mach number, flow direction and turbulent quantities were required as boundary conditions. The gauge pressure was set at 0 Pa. The velocities of the free air stream and the corresponding Mach numbers imposed at the boundary are summarized in Tab. 1. The table also presents the Reynolds numbers calculated based on airfoil chord length. As turbulent quantities, the turbulent kinetic energy, k, and the turbulent dissipation rate, ε, in the atmospheric boundary layer were specified. Their values are also presented in Tab. 1. The values of k and ε were calculated and corrected according to the formulas and remarks presented by Richards and Norris [7]. The aerodynamic roughness required to calculate k and ε was estimated at 1 based on the study of Grimmond et al. [8]. On the airfoils the usual no-slip condition was imposed.

The equations describing the flow, together with their boundary conditions, were integrated in space and time with the finite volume method implemented in the commercial code Ansys Fluent.

TABLE 1: Simulation parameters

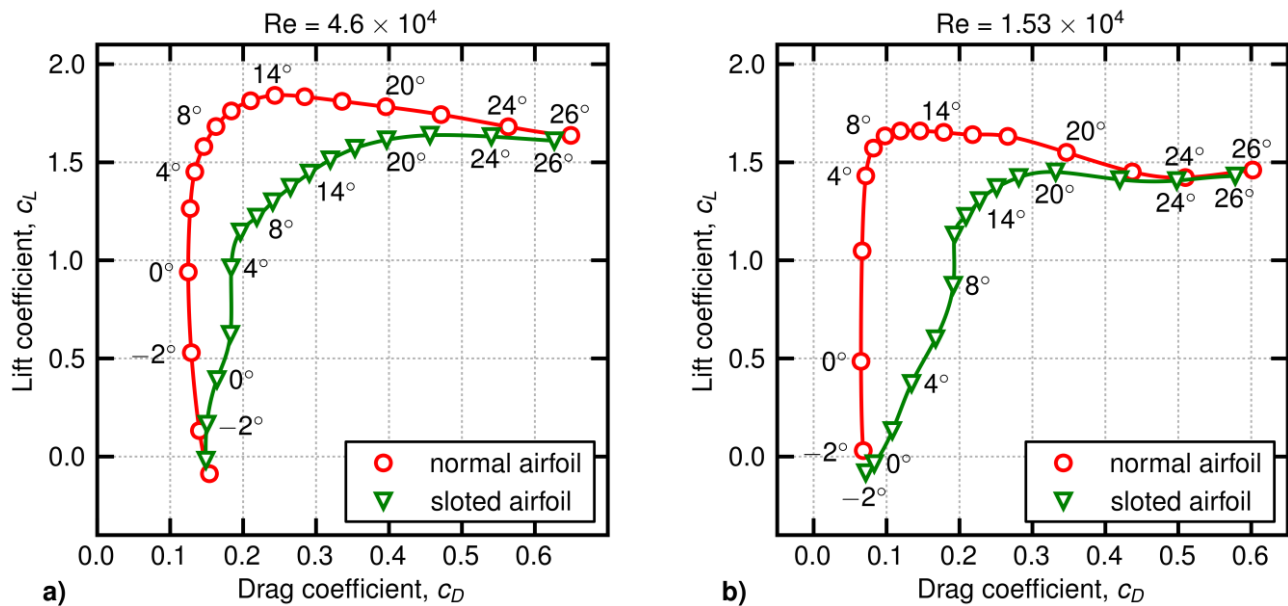| v_∞ (m/s)	Ma	Re	k (m^2/s^2)	ε (m^2/s^3)
3	8.7×10^{-3}	4.60×10^4	824	72
10	2.9×10^{-2}	1.53×10^5	9158	1337

Fig. 7. Comparisons of polar diagrams obtained numerically for both normal and slotted airfoil at a) Re = 4.6×10⁴ and b) Re = 1.53×10⁵.

Since only quadrilateral cells were used to mesh the computational domain, the QUICK scheme was chosen to discretize the flow equations in space. The discretization in time was accomplished with the first order implicit unsteady formulation.

For each airfoil, the first simulation was performed for the angle of attack of 0°. Subsequent simulations were carried out for angles of attack up to 26° and down to -4°. At each new simulation, the angle of attack was changed by 2° with respect to the previous simulation. The initial guess of each new simulation was the last converged solution of the previous simulation. Each simulation was advanced in time with a time step of 0.002 s until a stabilization of the lift and drag coefficients around an average value was observed for at least 30 s of the simulation time. At each time step, the convergence criterion was the drop in all scaled residuals below 10^{-4}.

The numerical results are summarized in Fig. 7 in form of polar diagrams of the normal and slotted airfoils at the two Reynolds numbers considered. It can be seen that, at low angles of attack, the slotted airfoil has a significantly lower lift than the normal airfoil. In the same time, the drag of the slotted airfoil increases. However, the drag remains about one order of magnitude lower than the lift. Therefore, in terms of absolute values, the decrease in lift is more important than the increase in drag. This behavior can be explained based on the pressure fields and flow configurations around the airfoils. Fig. 8 presents pressure fields and streamlines obtained for the angle of attack
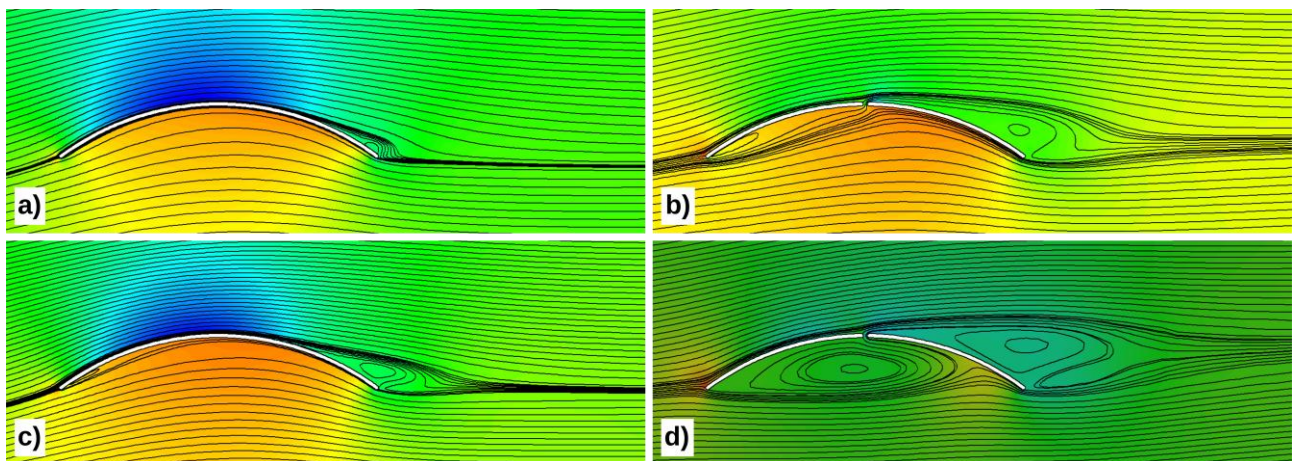

Fig. 8. Streamlines superimposed on pressure fields at $\alpha = 4°$: a) normal airfoil, Re = 4.6×10⁴, b) slotted airfoil, Re = 4.6×10⁴, c) normal airfoil, Re = 1.53×10⁵, d) slotted airfoil, Re = 1.53×10⁵.

$α = 4°$. It can be seen that, for both Reynolds numbers considered, the differences in pressure between pressure side and suction side of the slotted airfoil are clearly lower than in case of the normal airfoil. Hence, the lift of the slotted airfoil is lower. Additionally, the results suggest that the slot placed at mid-chord, with its axis perpendicular to camber line, favors the boundary layer separation, causing larger vortices both behind the slotted airfoil and below it, which could explain the increase in drag.

It is expected that the results presented in Fig. 7 and 8 will change to some extent when the airfoils will be arranged in a cascade. To assess the change, further research is required.

4. Conclusions

Experiments and numerical simulations show that circular arc-shaped airfoils with mid-chord slot have significantly lower lift and only slightly higher drag when compared with the un-slotted airfoils. The drag can be easily controlled by changing the slot width. Such airfoils can be used in applications where the decrease of the loads on wings or blades is desired in order to lower structural loads. A practical application is a cascade of guide vanes used to direct the air flow at appropriate absolute velocity angles towards the runner of a cross-flow wind turbine. This study can be extended in order to assess the influence of the cascade on the behavior of the slotted airfoils.

References

[1] H. Schlichting, K. Gersten, "Boundary Layer Theory", Springer, Berlin, 2000;
[2] A.L. Braslow, "A history of suction-type laminar-flow control with emphasis on flight research", Monographs in Aerospace History, No. 13, NASA History Division, Washington, 1999;
[3] A. Dragomirescu, "Performance assessment of a small wind turbine with crossflow runner by numerical simulations", Renewable Energy, 36, 2011, pp. 957–965;
[4] A. Dragomirescu, C.A. Safta and V. Serban, "A new type of crossflow runner for a small wind turbine", The 14th World Renewable Energy Congress – WREC2015, Bucharest, 2015;
[5] GUNT, Electronic 3-Component Measurement System, Technical book HM 170.40, 2002;
[6] Ansys Inc., "Ansys Fluent Theory Guide, Release 14.0", Canonsburg, 2011;
[7] P.J. Richards, S.E. Norris, "Appropriate boundary conditions for computational wind engineering models revisited", Journal of Wind Engineering and Industrial Aerodynamics, 99, 2011, pp. 257–266;
[8] C.S.B. Grimmond, T.S. King, M. Roth and T.R. Oke, "Aerodynamic roughness of urban areas derived from wind observations", Boundary-Layer Meteorology, 89, 1998, pp. 1–24.